

---

# Beyond Prioritized Replay: Sampling States in Model-Based RL via Simulated Priorities

---

Jincheng Mei & Yangchen Pan,\*Martha White  
University of Alberta  
jmei2,pan6,whitem@ualberta.ca

Amir-massoud Farahmand  
Vector Institute & University of Toronto  
farahmand@vectorinstitute.ai

Hengshuai Yao  
hengshuai@gmail.com

## Abstract

Model-based reinforcement learning (MBRL) can significantly improve sample efficiency, particularly when carefully choosing the states from which to sample hypothetical transitions. Such prioritization has been empirically shown to be useful for both experience replay (ER) and Dyna-style planning. However, there is as yet little theoretical understanding in RL about such prioritization strategies, and why they help. In this work, we revisit prioritized ER and, in an ideal setting, show an equivalence to minimizing cubic loss, providing theoretical insight into why it improves upon uniform sampling. This ideal setting, however, cannot be realized in practice, due to insufficient coverage of the sample space and outdated priorities of training samples. This motivates our model-based approach, which does not suffer from these limitations. Our key idea is to actively search for high priority states using gradient ascent. Under certain conditions, we prove that the distribution of hypothetical experiences generated from these states provides a diverse set of states, sampled proportionally to approximately true priorities. Our experiments on both benchmark and application-oriented domain show that our approach achieves superior performance over both the model-free prioritized ER method and several closely related model-based baselines.

## 1 Introduction

Using hypothetical experience simulated from an environment model can significantly improve sample efficiency of RL agents (Ha & Schmidhuber, 2018; Holland et al., 2018; Pan et al., 2018; van Hasselt et al., 2019). Dyna (Sutton, 1991) is a classical MBRL architecture where the agent uses real experience to update its policy as well as its reward and dynamics models. In-between taking actions, the agent can simulate hypothetical experience from the model to further improve the policy.

An important question for effective Dyna-style planning is *search-control*: from what states should the agent simulate hypothetical transitions? On each planning step in Dyna, the agent has to select a state and action from which to query the model for the next state and reward. This question, in fact, already arises in what is arguably the simplest variant of Dyna: Experience Replay (ER) (Lin, 1992). In ER, visited transitions are stored in a buffer and at each time step, a mini-batch of experiences is sampled to update the value function. ER can be seen as an instance of Dyna, using a (limited) non-parametric model given by the buffer (see van Seijen & Sutton (2015) for a deeper discussion). Performance can be significantly improved by sampling proportionally to priorities based on errors,

---

\*Equal contribution.

as in prioritized ER (Schaul et al., 2016; de Bruin et al., 2018), as well as specialized sampling for the off-policy setting (Schlegel et al., 2019).

Search-control strategies in Dyna similarly often rely on using priorities, though they can be more flexible in leveraging the model rather than being limited to only retrieving visited experiences. For example, a model enables the agent to sweep backwards by generating predecessors, as in prioritized sweeping (Moore & Atkeson, 1993; Sutton et al., 2008; Pan et al., 2018; Corneil et al., 2018). Other methods have tried alternatives to error-based prioritization, such as searching for states with high reward (Goyal et al., 2019), high value (Pan et al., 2019) or states that are difficult to learn (Pan et al., 2020). Another strategy has been to generate a more diverse set of states from which to sample (Gu et al., 2016; Holland et al., 2018), or to modulate the distance of such states from real experience (Janner et al., 2019). These methods are all supported by nice intuitions, but as yet lack solid theoretical reasons for why they can improve sample efficiency.

In this work, we provide new insights into how to choose the sampling distribution over states from which we generate hypothetical experience. In particular, we theoretically motivate why error-based prioritization is effective, and provide a mechanism to generate states according to more accurate error estimates. We first prove that  $l_2$  regression with error-based prioritized sampling is equivalent to minimizing a cubic objective with uniform sampling in an ideal setting. We then show that minimizing the cubic power objective has a faster convergence rate during early learning stage, providing theoretical motivation for error-based prioritization. We point out that this ideal setting is hard to achieve in practice using only ER due to two issues: insufficient sample space coverage and outdated priorities. Hence we propose a search-control strategy in Dyna that leverages a model to simulate errors and to find states with high expected error. Finally, we demonstrate the efficacy of our method on various benchmark domains and an autonomous driving application.

## 2 Problem Formulation

We formalize the problem as a Markov Decision Process (MDP), a tuple  $(\mathcal{S}, \mathcal{A}, \mathbb{P}, R, \gamma)$  including state space  $\mathcal{S}$ , action space  $\mathcal{A}$ , probability transition kernel  $\mathbb{P}$ , reward function  $R$ , and discount rate  $\gamma \in [0, 1]$ . At each environment time step  $t$ , an RL agent observes a state  $s_t \in \mathcal{S}$ , and takes an action  $a_t \in \mathcal{A}$ . The environment transitions to the next state  $s_{t+1} \sim \mathbb{P}(\cdot | s_t, a_t)$ , and emits a scalar reward signal  $r_{t+1} = R(s_t, a_t, s_{t+1})$ . A policy is a mapping  $\pi : \mathcal{S} \times \mathcal{A} \rightarrow [0, 1]$  that determines the probability of choosing an action at a given state.

The agent’s objective is to find an optimal policy. A popular algorithm is Q-learning (Watkins & Dayan, 1992), where parameterized action-values  $Q_\theta$  are updated using  $\theta = \theta + \alpha \delta_t \nabla_\theta Q_\theta(s_t, a_t)$  for step-size  $\alpha > 0$  with TD-error  $\delta_t \stackrel{\text{def}}{=} r_{t+1} + \gamma \max_{a' \in \mathcal{A}} Q_\theta(s_{t+1}, a') - Q_\theta(s_t, a_t)$ . The policy is defined by acting greedily w.r.t. these action-values. ER is critical when using neural networks to estimate  $Q_\theta$ , as used in DQN (Mnih et al., 2015), both to stabilize and speed up learning. MBRL has the potential to provide even further sample efficiency improvements.

We build on the Dyna formalism (Sutton, 1991) for MBRL, and more specifically the recently proposed HC-Dyna (Pan et al., 2019)

as shown in Algorithm 1. It is featured by a special Hill Climbing (HC)<sup>2</sup> search-control—the mechanism of generating states or state-action pairs from which to query the model to get next states and rewards (i.e. hypothetical experiences)—which generates states by hill climbing on some criterion function  $h(\cdot)$ . For example,  $h(\cdot)$  is the value function  $v(s)$  from Pan et al. (2019) and is the gradient

---

### Algorithm 1 HC-Dyna: Generic framework

---

**Input:** hill climbing crit.  $h : \mathcal{S} \mapsto \mathbb{R}$ , batch-size  $b$   
Initialize empty search-control queue  $B_{sc}$ ; empty ER buffer  $B_{er}$ ; initialize policy and model  $\mathcal{P}$   
**for**  $t = 1, 2, \dots$  **do**  
  Add  $(s_t, a_t, s_{t+1}, r_{t+1})$  to  $B_{er}$   
  **while** within some budget time steps **do**  
     $s \leftarrow s + \alpha_a \nabla_s h(s)$  //hill climbing  
    Add  $s$  into  $B_{sc}$   
  **for**  $n$  times **do**  
     $B \leftarrow \emptyset$   
    **for**  $b/2$  times **do**  
      Sample  $s \sim B_{sc}$ , on-policy action  $a$   
      Sample  $s', r \sim \mathcal{P}(s, a)$   
       $B \leftarrow (s, a, s', r)$   
    Sample  $b/2$  experiences from  $B_{er}$ , add to  $B$   
    Update policy on the mixed mini-batch  $B$

---

<sup>2</sup>The term Hill Climbing is used for generality as the vanilla gradient ascent procedure is modified to resolve certain challenges (Pan et al., 2019).

magnitude  $\|\nabla_s v(s)\|$  from Pan et al. (2020). The former is used as measure of “importance” of states and the latter is considered as a measure of value approximation difficulty.

These hypothetical transitions are treated just like real transitions. For this reason, HC-Dyna combines both real experience and hypothetical experience into mini-batch updates. These  $n$  updates, performed before taking the next action, are called planning updates, as they improve the action-value estimates—and so the policy—by a model.

### 3 A Deeper Look at Error-based Prioritized Sampling

In this section, we provide theoretical motivation for error-based prioritized sampling, and empirically investigate several insights highlighted by this theory. We show that prioritized sampling can be reformulated as optimizing a cubic power objective with uniform sampling. We prove that optimizing the cubic objective provides a faster convergence rate during early learning. Based on these results, we point out that for error-based prioritization, such as prioritized ER, to manifest advantages relies on up-to-date priorities and sufficient coverage of the sample space, and empirically highlight issues when those two properties are not obtained.

#### 3.1 Prioritized Sampling as a Cubic Objective

In  $l_2$  regression, we minimize the mean squared error  $\min_{\theta} \frac{1}{2n} \sum_{i=1}^n (f_{\theta}(x_i) - y_i)^2$ , for training set  $\mathcal{T} = \{(x_i, y_i)\}_{i=1}^n$  and function approximator  $f_{\theta}$ , such as a neural network. In error-based prioritized sampling, we define the priority of a sample  $(x, y) \in \mathcal{T}$  as  $|f_{\theta}(x) - y|$ ; the probability of drawing a sample  $(x, y) \in \mathcal{T}$  is typically  $q(x, y; \theta) \propto |f_{\theta}(x) - y|$ . We employ the following form to compute the probabilities:

$$q(x, y; \theta) \stackrel{\text{def}}{=} \frac{|f_{\theta}(x) - y|}{\sum_{i=1}^n |f_{\theta}(x_i) - y_i|} \quad (1)$$

We can show an equivalence between the gradients of the squared objective with this prioritization and the cubic power objective  $\frac{1}{3n} \sum_{i=1}^n |f_{\theta}(x_i) - y_i|^3$ . See Appendix A.2 for the proof.

**Theorem 1.** *For a constant  $c$  determined by  $\theta, \mathcal{T}$ , we have*

$$\mathbb{E}_{(x,y) \sim \text{uniform}(\mathcal{T})} [\nabla_{\theta} (1/3) |f_{\theta}(x) - y|^3] = c \mathbb{E}_{(x,y) \sim q(x,y;\theta)} [\nabla_{\theta} (1/2) (f_{\theta}(x) - y)^2]$$

This simple theorem provides an intuitive reason for why prioritized sampling can help improve sample efficiency: the gradient direction of cubic function is sharper than that of the square function when the error is relatively large (Figure 1). Theorem 2 further characterizes the difference between the convergence rates by optimizing the mean square error and the cubic power objective.

**Theorem 2** (Fast early learning). *Consider the following two objectives:  $\ell_2(x, y) \stackrel{\text{def}}{=} \frac{1}{2} (x - y)^2$ , and  $\ell_3(x, y) \stackrel{\text{def}}{=} \frac{1}{3} |x - y|^3$ . Denote  $\delta_t \stackrel{\text{def}}{=} |x_t - y|$ , and  $\tilde{\delta}_t \stackrel{\text{def}}{=} |\tilde{x}_t - y|$ . Define the functional gradient flow updates on these two objectives:*

$$\frac{dx_t}{dt} = -\eta \frac{d\{\frac{1}{2} (x_t - y)^2\}}{dx_t}, \quad \frac{d\tilde{x}_t}{dt} = -\eta \frac{d\{\frac{1}{3} |\tilde{x}_t - y|^3\}}{d\tilde{x}_t}. \quad (2)$$

*Given error threshold  $\epsilon \geq 0$ , define the hitting time  $t_{\epsilon} \stackrel{\text{def}}{=} \min_t \{t : \delta_t \leq \epsilon\}$  and  $\tilde{t}_{\epsilon} \stackrel{\text{def}}{=} \min_t \{t : \tilde{\delta}_t \leq \epsilon\}$ . For any initial function value  $x_0$  s.t.  $\delta_0 > 1$ ,  $\exists \epsilon_0 \in (0, 1)$  such that  $\forall \epsilon > \epsilon_0, t_{\epsilon} \geq \tilde{t}_{\epsilon}$ .<sup>3</sup>*

*Proof.* Please see Appendix A.3. Given the same  $\epsilon$  and the same initial value of  $x$ , first we derive  $t_{\epsilon} = \frac{1}{\eta} \cdot \ln \left\{ \frac{\delta_0}{\epsilon} \right\}$ ,  $\tilde{t}_{\epsilon} = \frac{1}{\eta} \cdot \left( \frac{1}{\epsilon} - \frac{1}{\delta_0} \right)$ . Then we analyze the condition on  $\epsilon$  to see when  $t_{\epsilon} \geq \tilde{t}_{\epsilon}$ , i.e. minimizing the square error is slower than minimizing the cubic error.  $\square$

The above theorem says that when the initial error is relatively large, it is faster to get to a certain low error point with the cubic objective. We can test this in simulation, with the following minimization

<sup>3</sup>Finding the exact value of  $\epsilon_0$  would require a definition of ordering on complex plane, which leads to  $\epsilon_0 = -\frac{1}{W(\log 1/a - 1/a - \pi i)}$  and  $W(\cdot)$  is a Wright Omega function, then we have  $\tilde{t}_{\epsilon} \leq t_{\epsilon}$ . Our theorem statement is sufficient for the purpose of characterizing convergence rate.

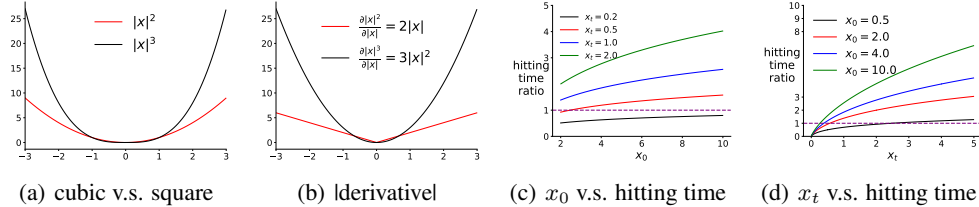


Figure 1: (a) show cubic v.s. square function. (b) shows their absolute derivatives. (c) shows the hitting time ratio v.s. initial value  $x_0$  under different target value  $x_t$ . (d) shows the ratio v.s. the target  $x_t$  to reach under different  $x_0$ . Note that a ratio larger than 1 indicates a longer time to reach the given  $x_t$  for the square loss.

problems:  $\min_{x \geq 0} x^2$  and  $\min_{x \geq 0} x^3$ . We use the hitting time formulae  $t_\epsilon = \frac{1}{\eta} \cdot \ln \left\{ \frac{\delta_0}{\epsilon} \right\}$ ,  $\tilde{t}_\epsilon = \frac{1}{\eta} \cdot \left( \frac{1}{\epsilon} - \frac{1}{\delta_0} \right)$  derived in the proof, to compute the hitting time ratio  $\frac{t_\epsilon}{\tilde{t}_\epsilon}$  under different initial values  $x_0$  and final error value  $\epsilon$ . In Figure 1(c)(d), we can see that it usually takes a significantly shorter time for the cubic loss to reach a certain  $x_t$  with various  $x_0$  values.

### 3.2 Empirical Demonstrations

In this section, we empirically show: 1) the practical performance of cubic objective; 2) the importance of sufficient sample space coverage and of updating priorities of all training samples; 3) the reasons for why high power objective should not be preferred in general. We refer readers to A.6 for missing details and to A.7 for additional experiments.

We conduct experiments on a supervised learning task. We use the dataset from Pan et al. (2020), where it is shown that the high frequency region  $[-2, 0]$  is the main source of prediction error. Hence we expect prioritized sampling to make a clear difference in terms of sample efficiency. We generate a training set  $\mathcal{T}$ ,  $|\mathcal{T}| = 4000$  by uniformly sampling  $x \in [-2, 2]$  and adding zero-mean Gaussian noise with standard deviation  $\sigma$  to the target  $f_{\sin}(x)$  values, where  $f_{\sin}(x) = \sin(8\pi x)$  if  $x \in [-2, 0]$  and  $f_{\sin}(x) = \sin(\pi x)$  if  $x \in [0, 2]$ . The testing set contains 1k samples and the targets are not noise-contaminated.

We compare the following algorithms. **L2**: the  $l_2$  regression with uniformly sampling from  $\mathcal{T}$ . **Full-PrioritizedL2**: the  $l_2$  regression with prioritized sampling according to the distribution defined in (1), the priorities of *all samples* in the training set are updated after each mini-batch update. **PrioritizedL2**: the only difference with **Full-PrioritizedL2** is that *only* the priorities of those training examples sampled in the mini-batch are updated at each iteration, the rest of the training samples keep the original priorities. Note that this resembles what the vanilla Prioritized ER does in RL setting (Schaul et al., 2016). **Cubic**: minimizing the cubic objective with uniformly sampling. **Power4**:  $\min_{\theta} \frac{1}{n} \sum_{i=1}^n (f_{\theta}(x_i) - y_i)^4$  with uniformly sampling. We include it to show that there is almost no gain and may get hurt by using higher powers.

We use  $32 \times 32$  tanh layers for all algorithms and optimize learning rate from the range  $\{0.01, 0.001, 0.0001\}$ . Figure 2 (a)-(d) show the learning curves in terms of testing error of all the above algorithms with various settings.<sup>4</sup> We identify five important observations: 1) with a small mini-batch size 128, there is a significant difference between **Full-PrioritizedL2** and **Cubic**; 2) with increased mini-batch size, although all algorithms perform better, **Cubic** achieves largest improvement and its behavior tends to approximate the prioritized sampling algorithm; 3) as shown in Figure 2 (a), the prioritized sampling does not show advantage when the training set is small; 4) Prioritized  $l_2$  without updating all priorities can be significantly worse than the vanilla (uniform sampling)  $l_2$  regression; 5) when increasing noise standard deviation  $\sigma$  from 0.1 to 0.5, all algorithms perform worse and the *higher power* the objective is, the *more* it can get hurt.

**The importance of sample space coverage.** Observation 1) and 2) show that high power objective has to use a much larger mini-batch size to achieve comparable performance with the  $l_2$  with prioritized sampling. Though this coincides with Theorem 1 in that the two algorithms is equivalent in expectation, prioritized sampling seems to be robust to small mini-batch, which is an advantage in stochastic gradient methods. A possible reason is that prioritized sampling allows to immediately get

<sup>4</sup>We show the testing error as it is finally concerned. The training error has similar comparative performance and is presented in Appendix 3, where we also include additional results with different settings.

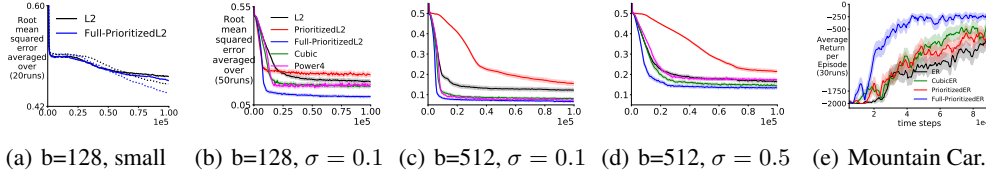


Figure 2: Testing RMSE v.s. number of mini-batch updates. (a)(b)(c)(d) show the learning curves with different mini-batch size  $b$  or Gaussian noises variance  $\sigma$  added to the training targets. (a) is using  $\sigma = 0.1$  and a smaller training set (solid line for  $|\mathcal{T}| = 800$ , dotted line for  $|\mathcal{T}| = 1600$ ) than others but has the same testing set size. (e) shows the a corresponding experiment in RL setting on the classical mountain car domain. The results are averaged over 50 random seeds on (a)-(d) and 30 on (e). The shade indicates standard error.

many samples from those high error region; while uniformly sampling can get fewer those samples with limited mini-batch size. This motivates us to test prioritized sampling with a small training set where both algorithms can get fewer samples everywhere. Figure 2(a) together with (b) indicate that prioritized sampling needs sufficient samples across the sample space to maintain advantage. This requirement is intuitive but it illuminates an important limitation of prioritized ER in RL: only those visited real experiences from the ER buffer can get sampled. If the state space is large, the ER buffer likely contains only a small subset of the state space, indicating a very small training set.

**Thorough priority updating.** Observation 4) reminds us the importance of using an up-to-date sampling distribution at each time step. Outdated priorities change the sampling distribution in an unpredictable manner and the learning performance can get hurt. Though the effect of whether updating priorities of all samples or not is intuitive, it receives little attention in the existing RL literature. We further verify this phenomenon on the classical Mountain Car domain (Sutton & Barto, 2018; Brockman et al., 2016). Figure 2(e) shows the evaluation learning curves of different variants of Deep Q networks (DQN) corresponding to the supervised learning algorithms. We use a small  $16 \times 16$  ReLU NN as the  $Q$ -function. We expect that a small NN should highlight the issue of priority updating: every mini-batch update potentially perturbs the values of many other states. Hence it is likely that many experiences in the ER buffer have the wrong priorities without thorough priority updating. One can see that Full-PrioritizedER significantly outperforms the vanilla PrioritizedER algorithm which only updates priorities for those in the sampled mini-batch at each time step. However, updating the priorities of all samples at each time step in the ER buffer is usually computationally too expensive and is not scalable to number of visited samples.

**Regarding high power objectives.** As we discussed above, observation 1) and 2) tell us that that high power objective would require a large mini-batch size (ideally, use a batch algorithm, i.e. the whole training set) to manifest the advantage in improving convergence rate. This makes the algorithm not easily scalable to large training dataset. Observation 5) indicates another reason for why a high power objective should not be preferred: it augments the effect of noise added to the target variables. In Figure 2(d), the Power4 objective suffers most from the increased target noise.

## 4 Acquiring Samples From Temporal Difference Error-based Sampling Distribution on Continuous Domains

In this section, we propose a method attempting to sample states: 1) which are not restricted to those visited ones; 2) with probability proportional to the expected TD error magnitude and the probability is computed according to  $Q$ -function parameters at current time step (i.e. this typically would require to compute priorities of all samples at each time step). We start by the following theorem. We denote  $\mathbb{P}^\pi(s', r|s)$  as the transition probability given a policy  $\pi$ .

**Theorem 3. Sampling method.** Given the state  $s \in \mathcal{S}$ , let  $v^\pi(\cdot; \theta) : \mathcal{S} \mapsto \mathbb{R}$  be a differentiable value function under policy  $\pi$  parameterized by  $\theta$ . Define:  $y(s) \stackrel{\text{def}}{=} \mathbb{E}_{r, s' \sim \mathcal{P}^\pi(s', r|s)} [r + \gamma v^\pi(s'; \theta)]$ , and denote the TD error as  $\delta(s, y; \theta_t) \stackrel{\text{def}}{=} y(s) - v(s; \theta_t)$ . Given some initial state  $s_0 \in \mathcal{S}$ , define the state sequence  $\{s_i\}$  as the one generated by state updating rule  $s_{i+1} \leftarrow s_i + \alpha_a \nabla_s \log |\delta(s_i, y(s_i); \theta_t)| + X_i$ , where  $\alpha_a$  is a sufficiently small stepsize and  $X_i$  is a Gaussian random variable with a sufficiently small variance. Then the sequence  $\{s_i\}$  converges to the distribution  $p(s) \propto |\delta(s, y(s))|$ .



The proof is a direct consequence of the convergent behavior of Langevin dynamics stochastic differential equation (SDE)(Roberts, 1996; Welling & Teh, 2011; Zhang et al., 2017). We include a brief discussion and background knowledge in the Appendix A.4.

In practice, we can compute the state value estimate by  $v(s) = \max_a Q(s, a; \theta_t)$  as suggested by Pan et al. (2019). In the case that a true environment model is not available, we have to compute an estimate  $\hat{y}(s)$  of  $y(s)$  by a learned model. Then at each time step  $t$ , states approximately following the distribution  $p(s) \propto |\delta(s, y(s))|$  can be generated by

$$s \leftarrow s + \alpha_a \nabla_s \log |\hat{y}(s) - \max_a Q(s, a; \theta_t)| + X, \quad (3)$$

where  $X$  is a Gaussian random variable with zero-mean and reasonably small variance. In implementation, observing that  $\alpha_a$  is small, we opt to consider  $\hat{y}(s)$  as a constant given a state  $s$  without backpropagating through it. We provide an upper bound in the following theorem for the difference between the sampling distribution acquired by the true model and the learned model. We denote the transition probability distribution under policy  $\pi$  and the true model as  $\mathcal{P}^\pi(r, s'|s)$ ; denote that with the learned model as  $\hat{\mathcal{P}}^\pi(r, s'|s)$ . Let  $p(s)$  and  $\hat{p}(s)$  be the convergent distributions described in Theorem 3 by using true and learned models respectively. Let  $d_{tv}(\cdot, \cdot)$  be the total variation distance between two probability distributions. Define  $u(s) \stackrel{\text{def}}{=} |\delta(s, y(s))|$ ,  $\hat{u}(s) \stackrel{\text{def}}{=} |\delta(s, \hat{y}(s))|$ ,  $Z \stackrel{\text{def}}{=} \int_{s \in \mathcal{S}} u(s) ds$ ,  $\hat{Z} \stackrel{\text{def}}{=} \int_{s \in \mathcal{S}} \hat{u}(s) ds$ .

**Theorem 4.** Assume: 1) the reward magnitude is bounded  $|r| \leq R_{max}$  and define  $V_{max} \stackrel{\text{def}}{=} \frac{R_{max}}{1-\gamma}$ ; 2) the largest model error for a single state is some small value:  $\epsilon_s \stackrel{\text{def}}{=} \max_s d_{tv}(\mathcal{P}^\pi(\cdot|s), \hat{\mathcal{P}}^\pi(\cdot|s))$ . Then  $\forall s \in \mathcal{S}$ ,  $|p(s) - \hat{p}(s)| \leq \max(\frac{u(s)+V_{max}\epsilon_s}{Z} - p(s), \frac{\hat{u}(s)+V_{max}\epsilon_s}{\hat{Z}} - \hat{p}(s))$ .

Please see Appendix A.5 for proof.

**Algorithmic details.** We present the key details of our algorithm called Dyna-TD (Temporal Difference error) in the Algorithm 3 in Appendix A.6. The algorithm closely follows the previous hill climbing Dyna by Pan et al. (2019). At each time step, we run the updating rule 3 and record the states along the gradient trajectories to populate the search-control queue. Then during planning stage, we sample states from the search-control queue and pair them with on-policy actions to get state-action pairs. We query the model those state-action pairs to acquire corresponding next states, rewards to acquire hypothetical experiences in the form of  $(s_t, a_t, s_{t+1}, r_{t+1})$ . Then we mix those hypothetical experiences with real experiences from the ER buffer to form a mixed mini-batch to update the NN parameters.

**Empirical verification of sampling distribution.** We validate the efficacy of our sampling method by empirically examining the distance between the sampling distribution acquired by our gradient ascent rule (3) (denoted as  $p_1(\cdot)$ ) and the desired distribution computed by thorough priority updating  $p^*(\cdot)$  of all states under the current parameter on the GridWorld domain (Pan et al., 2019) (Figure 3(a)), where the probability density can be conveniently approximated by discretization. We record the distance change when we train our Algorithm 3. The distance between the sampling distribution for Prioritized ER (denoted as  $p_2(\cdot)$ ) is also included for comparison. All those distributions are computed by normalizing visitation counts on the discretized  $50 \times 50$  GridWorld. We compute the distances of  $p_1, p_2$  to  $p^*$  by two sensible weighting schemes: 1) on-policy weighting:  $\sum_{j=1}^{2500} d^\pi(s_j) |p_i(s_j) - p^*(s_j)|$ ,  $i \in \{1, 2\}$ , where  $d^\pi$  is approximated by uniformly sample 3k states from a recency buffer; 2) uniform weighting:  $\frac{1}{2500} \sum_{j=1}^{2500} |p_i(s_j) - p^*(s_j)|$ ,  $i \in \{1, 2\}$ . All details are in Appendix A.6

Figure 3(b)(c) show that our algorithm Dyna-TD, either with a true or an online learned model, maintains a significantly closer distance to the desired sampling distribution  $p^*$  than PrioritizedER under both weighting schemes. Furthermore, despite there is mismatch between implementation and our above Theorem 3 in that Dyna-TD may not run enough gradient steps to reach stationary distribution, the induced sampling distribution is quite close to the one by running a long gradient steps (Dyna-TD-Long), which is closer to the theorem. This indicates that we can reduce time cost by lowering the number of gradient steps, while keep the sampling distribution similar.

## 5 Experiments

In this section, we empirically show that our algorithm achieves stable and consistent performances across different settings. We firstly show the overall comparative performances on various benchmark

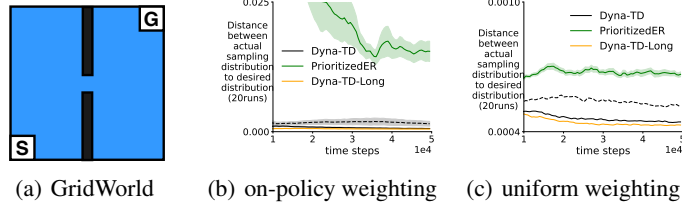


Figure 3: (a) shows the GridWorld taken from Pan et al. (2019). The state space is  $\mathcal{S} = [0, 1]^2$ , and the agent starts from the left bottom and should learn to take action from  $\mathcal{A} = \{up, down, right, left\}$  to reach the right top within as few steps as possible. (b) shows the distance change as a function of training steps. The **dashed** line corresponds to our algorithm with an online learned model. The corresponding evaluation learning curve is in the Figure 4(c). All results are averaged over 20 random seeds and the shade indicates standard error.

domains. We then show that our algorithm **Dyna-TD** is more robust to environment noise than PrioritizedER. Last, we demonstrate the practical utility of our algorithm on an autonomous driving vehicle application. Note that our Dyna-TD keeps using the same hill climbing parameter setting across all benchmark domains. We refer readers to the Appendix A.6 for any missing details.

**Baselines.** We include the following baseline competitors. **ER** is the DQN with a regular ER buffer without prioritized sampling. **PrioritizedER** is using a priority queue to store visited experiences and each experience is sampled proportional to its TD error magnitude. Note that according to the original paper (Schaul et al., 2016), after each mini-batch update, only the priorities of those samples in the mini-batch are updated. **Dyna-Value** (Pan et al., 2019) is the Dyna variant which performs hill climbing on value function to acquire states to populate the search-control queue. **Dyna-Frequency** (Pan et al., 2020) is the Dyna variant which performs hill climbing on the norm of the gradient of the value function to acquire states to populate the search-control queue.

**Overall Performances.** Figure 4 shows the overall performances of different algorithms on Acrobot, CartPole, GridWorld (Figure 3(a)) and MazeGridWorld (Figure 4(g)). Our key observations are: 1) Dyna-Value or Dyna-Frequency may converge to a sub-optimal policy when using a large number of planning steps; 2) Dyna-Frequency has clearly inconsistent performances across different domains; 3) our algorithm performs the best in most cases; and even with an online learned model, our algorithm outperforms others on most of the tasks; 4) in most cases, model-based methods (Dyna-) significantly outperform model-free methods.

Our interpretations of those observations are as following. First, for Dyna-Value, think about the case where some states have high value but low TD error, the valued-based hill climbing methods may still frequently acquire those states and this can waste of samples and meanwhile incurs sampling distribution bias which leads to a sub-optimal policy. This sub-optimality can be clearly observed on Acrobot, GridWorld and MazeGridWorld. Similar reasoning applies to Dyna-Frequency. Second, for Dyna-Frequency, as indicated by the original paper Pan et al. (2020), the gradient or hessian norm have very different numerical scales and highly depends on the choice of the function approximator or domain, this indicates that the algorithm requires finely tuned parameter setting as testing domain varies, which possibly explains its inconsistent performances across domains. Furthermore, the Hessian-gradient product can be expensive and we observe Dyna-Frequency takes much longer time to run the experiment than other Dyna variants. Third, since we fetch the same number of states during the search-control process for all Dyna variants, the superior performance of our Dyna-TD indicates the utility of the samples acquired by our approach. Fourth, notice that each algorithm runs the same number of planning steps, while model-based algorithms perform significantly better, this indicates the benefits of leveraging the generalization power of the learned value function. In contrast, model-free methods can only utilize visited states.

**Robustness to Noise.** As a correspondent experiment to the supervised learning setting in Section 3, we show that our algorithm is more robust to increased noise variance than the prioritized ER. Figure 5 show the evaluation learning curves on Mountain Car with planning steps 10, 30 and reward noise standard deviation  $\sigma \in \{0, 0.1\}$ . We would like to identify three key observations. First, our algorithm’s relative performance to PrioritizedER resembles the Full-PrioritizedL2 to PrioritizedL2 from the supervised learning setting, as Full-PrioritizedL2 is more robust to target noise than PrioritizedL2. Second, our algorithm achieves almost the same performance as Dyna-Frequency which is claimed to be robust to noise by Pan et al. (2020). Last, as observed on other environments, usually all algorithms can benefit from the increased number of planning steps;

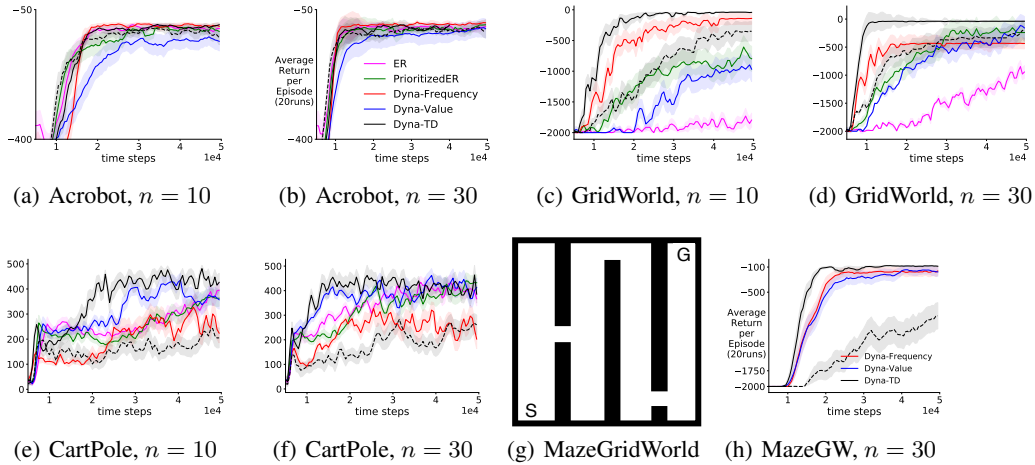


Figure 4: Evaluation learning curves on benchmark domains with planning updates  $n = 10, 30$ . The **dashed** line denotes Dyna-TD with an online learned model. All results are averaged over 20 random seeds. Figure(g) shows MazeGridWorld(GW) taken from Pan et al. (2020) and the learning curves are in (h).

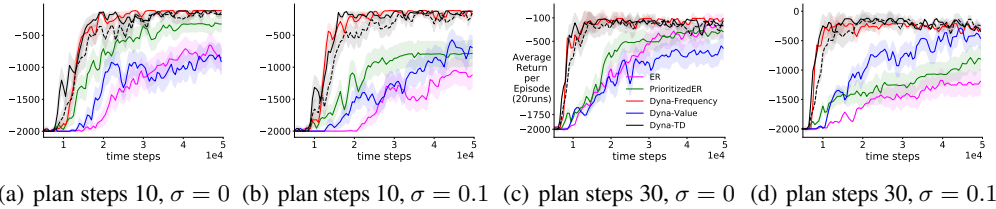


Figure 5: Evaluation learning curves on Mountain Car with different number of planning updates and different reward noise variance. At each time step, the reward is sampled from the Gaussian  $N(-1, \sigma)$ .  $\sigma = 0$  indicates deterministic reward. All results are averaged over 20 random seeds.

however, the PrioritizedER and ER get clearly hurt when using more planning steps with the noise presented, this illuminates the limitation of the model-free methods.

**Practical Utility in Autonomous Driving Application.** We study the practical utility of our method in an autonomous driving application (Leurent, 2018) with an online learned model. As shown in Figure 6 (a), we test on the roundabout-v0 domain, where the agent (i.e. the green car) should learn to go through a roundabout without collisions while maintaining as high speed as possible. We would like to emphasize that the domains are not difficult to train to reach some near optimal policy; this can be seen from the previous work by Leurent et al. (2019), which shows that different algorithms achieve similar episodic return. However, we observe that there is a significantly lower number of car crashes with the policy learned by our algorithm on both domains as we show in Figure 6(b). This coincides with our intuition—the crash should incur high temporal difference error and our method of actively searching such states by gradient ascent should make the agent get sufficient training during planning stage, hence the agent can better handle these scenarios than model-free methods.

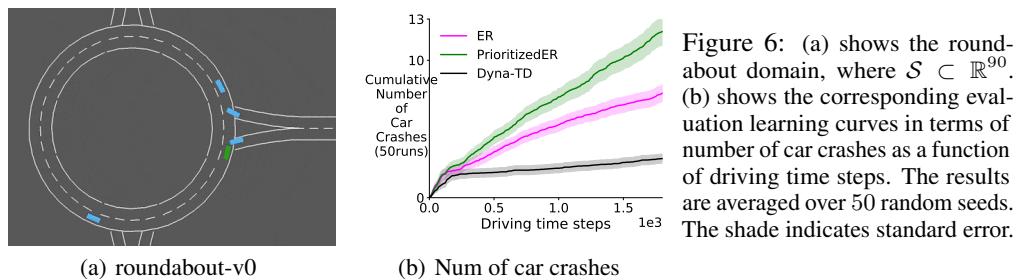


Figure 6: (a) shows the roundabout domain, where  $S \subset \mathbb{R}^{90}$ . (b) shows the corresponding evaluation learning curves in terms of number of car crashes as a function of driving time steps. The results are averaged over 50 random seeds. The shade indicates standard error.



## 6 Discussion

In this work, we provide theoretical reason for why prioritized ER can help improve sample efficiency. We identify crucial factors for it to be effective: sample space coverage and thorough priority updating. We then propose to sample states by Langevine dynamics and conduct experiments to show the efficacy of our method. Interesting future directions include: 1) studying the effect of model error in sample efficiency with our search control; 2) applying our method with a feature-to-feature model, which can improve scalability of our method.

## 7 Broader Impact Discussion

This work is about methodology of how to efficiently sample hypothetical experiences in model-based reinforcement learning. Potential impact of this work is likely to be further improvement of sample efficiency of reinforcement learning methods, which should be generally beneficial to the reinforcement learning research community. We have not considered specific applications or scenarios as the goal of this work.

## References

- Abadi, M., Agarwal, A., Barham, P., Brevdo, E., Chen, Z., and et al. TensorFlow: Large-scale machine learning on heterogeneous systems. *Software available from tensorflow.org*, 2015.
- Brockman, G., Cheung, V., Pettersson, L., Schneider, J., Schulman, J., Tang, J., and Zaremba, W. OpenAI Gym. arXiv:1606.01540, 2016.
- Chiang, T.-S., Hwang, C.-R., and Sheu, S. J. Diffusion for global optimization in  $\mathbb{R}^n$ . *SIAM Journal on Control and Optimization*, pp. 737–753, 1987.
- Cornell, D. S., Gerstner, W., and Brea, J. Efficient model-based deep reinforcement learning with variational state tabulation. In *International Conference on Machine Learning*, pp. 1049–1058, 2018.
- de Bruin, T., Kober, J., Tuyls, K., and Babuska, R. Experience selection in deep reinforcement learning for control. *Journal of Machine Learning Research*, 2018.
- Durmus, A. and Moulines, E. Nonasymptotic convergence analysis for the unadjusted Langevin algorithm. *The Annals of Applied Probability*, pp. 1551–1587, 2017.
- Fanaee-T, H. and Gama, J. Event labeling combining ensemble detectors and background knowledge. *Progress in Artificial Intelligence*, pp. 1–15, 2013.
- Glorot, X. and Bengio, Y. Understanding the difficulty of training deep feedforward neural networks. In *International Conference on Artificial Intelligence and Statistics*, 2010.
- Goyal, A., Brakel, P., Fedus, W., Singhal, S., Lillicrap, T., Levine, S., Larochelle, H., and Bengio, Y. Recall traces: Backtracking models for efficient reinforcement learning. In *International Conference on Learning Representations*, 2019.
- Gu, S., Lillicrap, T. P., Sutskever, I., and Levine, S. Continuous Deep Q-Learning with Model-based Acceleration. In *International Conference on Machine Learning*, pp. 2829–2838, 2016.
- Ha, D. and Schmidhuber, J. Recurrent world models facilitate policy evolution. *Advances in Neural Information Processing Systems*, pp. 2450–2462, 2018.
- Holland, G. Z., Talvitie, E., and Bowling, M. The effect of planning shape on dyna-style planning in high-dimensional state spaces. *CoRR*, abs/1806.01825, 2018.
- Janner, M., Fu, J., Zhang, M., and Levine, S. When to trust your model: Model-based policy optimization. *Advances in Neural Information Processing Systems*, pp. 12519–12530, 2019.
- Kingma, D. and Ba, J. Adam: A method for stochastic optimization. *International Conference on Learning Representations*, 12 2014.
- Leurent, E. An environment for autonomous driving decision-making. <https://github.com/eleurent/highway-env>, 2018.

- Leurent, E., Blanco, Y., Efimov, D., and Maillard, O. Approximate robust control of uncertain dynamical systems. *CoRR*, abs/1903.00220, 2019.
- Lin, L.-J. Self-Improving Reactive Agents Based On Reinforcement Learning, Planning and Teaching. *Machine Learning*, 1992.
- Mnih, V., Kavukcuoglu, K., Silver, D., Rusu, A. A., Veness, J., Bellemare, M. G., Graves, A., Riedmiller, M., Fidjeland, A. K., Ostrovski, G., Petersen, S., Beattie, C., Sadik, A., Antonoglou, I., King, H., Kumaran, D., Wierstra, D., Legg, S., and Hassabis, D. Human-level control through deep reinforcement learning. *Nature*, 2015.
- Moore, A. W. and Atkeson, C. G. Prioritized sweeping: Reinforcement learning with less data and less time. *Machine learning*, pp. 103–130, 1993.
- Pan, Y., Zaheer, M., White, A., Patterson, A., and White, M. Organizing experience: a deeper look at replay mechanisms for sample-based planning in continuous state domains. In *International Joint Conference on Artificial Intelligence*, pp. 4794–4800, 2018.
- Pan, Y., Yao, H., Farahmand, A.-m., and White, M. Hill climbing on value estimates for search-control in dyna. In *International Joint Conference on Artificial Intelligence*, 2019.
- Pan, Y., Mei, J., and massoud Farahmand, A. Frequency-based search-control in dyna. In *International Conference on Learning Representations*, 2020.
- Roberts, Gareth O. and Tweedie, R. L. Exponential convergence of langevin distributions and their discrete approximations. *Bernoulli*, pp. 341–363, 1996.
- Schaul, T., Quan, J., Antonoglou, I., and Silver, D. Prioritized Experience Replay. In *International Conference on Learning Representations*, 2016.
- Schlegel, M., Chung, W., Graves, D., Qian, J., and White, M. Importance resampling for off-policy prediction. *Advances in Neural Information Processing Systems 32*, pp. 1799–1809, 2019.
- Sutton, R. S. Integrated architectures for learning, planning, and reacting based on approximating dynamic programming. In *ML*, 1990.
- Sutton, R. S. Integrated modeling and control based on reinforcement learning and dynamic programming. In *Advances in Neural Information Processing Systems*, 1991.
- Sutton, R. S. and Barto, A. G. *Reinforcement Learning: An Introduction*. The MIT Press, second edition, 2018.
- Sutton, R. S., Szepesvári, C., Geramifard, A., and Bowling, M. Dyna-style planning with linear function approximation and prioritized sweeping. In *UAI*, pp. 528–536, 2008.
- van Hasselt, H. P., Hessel, M., and Aslanides, J. When to use parametric models in reinforcement learning? In *Advances in Neural Information Processing Systems*, pp. 14322–14333, 2019.
- van Seijen, H. and Sutton, R. S. A deeper look at planning as learning from replay. In *International Conference on Machine Learning*, pp. 2314–2322, 2015.
- Watkins, C. J. C. H. and Dayan, P. Q-learning. *Machine Learning*, pp. 279–292, 1992.
- Welling, M. and Teh, Y. W. Bayesian learning via stochastic gradient Langevin dynamics. In *International Conference on Machine Learning*, pp. 681–688, 2011.
- Zhang, Y., Liang, P., and Charikar, M. A hitting time analysis of stochastic gradient langevin dynamics. In *Conference on Learning Theory*, pp. 1980–2022, 2017.

## A Appendix

In Section A.1, we introduce some background in Dyna architecture. We then provide the full proof of Theorem 2 in Section A.3. We briefly discuss Langevin dynamics in Section A.4, and present the proof for Theorem 4 in Section A.5. Details for reproducible research are in Section A.6. We provide supplementary experimental results in Section A.7.

### A.1 Background in Dyna

Dyna integrates model-free and model-based policy updates in an online RL setting (Sutton, 1990). As shown in Algorithm 2, at each time step, a Dyna agent uses the real experience to learn a model and performs model-free policy update. During the *planning* stage, simulated experiences are acquired from the model to further improve the policy. It should be noted that the concept of planning refers to any computational process which leverages a model to improve policy, according to Sutton & Barto (2018). The mechanism of generating states or state-action pairs from which to query the model is called *search-control*, which is of critical importance to the sample efficiency. There are abundant existing works (Moore & Atkeson, 1993; Sutton et al., 2008; Gu et al., 2016; Pan et al., 2018; Corneil et al., 2018; Goyal et al., 2019; Janner et al., 2019; Pan et al., 2019) report different level of sample efficiency improvements by using different way of generating hypothetical experiences during the planning stage.

---

#### Algorithm 2 Tabular Dyna

---

```

Initialize  $Q(s, a)$ ; initialize model  $\mathcal{M}(s, a), \forall (s, a) \in \mathcal{S} \times \mathcal{A}$ 
while true do
  observe  $s$ , take action  $a$  by  $\epsilon$ -greedy w.r.t  $Q(s, \cdot)$ 
  execute  $a$ , observe reward  $R$  and next State  $s'$ 
  Q-learning update for  $Q(s, a)$ 
  update model  $\mathcal{M}(s, a)$  (i.e. by counting)
  store  $(s, a)$  into search-control queue
  for  $i=1:d$  do
    sample  $(\tilde{s}, \tilde{a})$  from search-control queue
     $(\tilde{s}', \tilde{R}) \leftarrow \mathcal{M}(\tilde{s}, \tilde{a})$  // simulated transition
    Q-learning update for  $Q(\tilde{s}, \tilde{a})$  // planning update

```

---

### A.2 Proof for Theorem 1

**Theorem 1.** For a constant  $c$  determined by  $\theta, \mathcal{T}$ , we have

$$\mathbb{E}_{(x,y) \sim \text{uniform}(\mathcal{T})}[\nabla_{\theta}(1/3)|f_{\theta}(x) - y|^3] = c\mathbb{E}_{(x,y) \sim q(x,y;\theta)}[\nabla_{\theta}(1/2)(f_{\theta}(x) - y)^2]$$

*Proof.* The proof is very intuitive. The expected gradient of the uniform sampling method is

$$\begin{aligned} \mathbb{E}_{(x,y) \sim \text{uniform}(\mathcal{T})}[\nabla_{\theta}(1/3)|f_{\theta}(x) - y|^3] &= \frac{1}{n} \sum_{i=1}^n |f_{\theta}(x_i) - y_i| \nabla_{\theta}(f_{\theta}(x_i) - y_i)^2 \\ \mathbb{E}_{(x,y) \sim q(x,y;\theta)}[\nabla_{\theta}(1/2)(f_{\theta}(x) - y)^2] &= \sum_{i=1}^n q(x_i, y_i; \theta) \nabla_{\theta}(f_{\theta}(x_i) - y_i)^2 \\ &= \frac{1}{\sum_{i=1}^n |f_{\theta}(x_i) - y_i|} \sum_{i=1}^n |f_{\theta}(x_i) - y_i| \nabla_{\theta}(f_{\theta}(x) - y)^2 \\ &= \frac{n}{\sum_{i=1}^n |f_{\theta}(x_i) - y_i|} \mathbb{E}_{(x,y) \sim \text{uniform}(\mathcal{T})}[\nabla_{\theta}(1/3)|f_{\theta}(x) - y|^3] \end{aligned}$$

Setting  $c = \frac{\sum_{i=1}^n |f_{\theta}(x_i) - y_i|}{n}$  completes the proof.  $\square$

### A.3 Proof for Theorem 2

**Theorem 2.** Consider the following two objectives:  $\ell_2(x, y) \stackrel{\text{def}}{=} \frac{1}{2}(x - y)^2$ , and  $\ell_3(x, y) \stackrel{\text{def}}{=} \frac{1}{3}|x - y|^3$ . Denote  $\delta_t \stackrel{\text{def}}{=} |x_t - y|$ , and  $\tilde{\delta}_t \stackrel{\text{def}}{=} |\tilde{x}_t - y|$ . Define the functional gradient flow updates on these two objectives:

$$\frac{dx_t}{dt} = -\eta \frac{d\{\frac{1}{2}(x_t - y)^2\}}{dx_t}, \quad \frac{d\tilde{x}_t}{dt} = -\eta \frac{d\{\frac{1}{3}|\tilde{x}_t - y|^3\}}{d\tilde{x}_t}. \quad (4)$$

Given error threshold  $\epsilon \geq 0$ , define the hitting time  $t_\epsilon \stackrel{\text{def}}{=} \min_t \{t : \delta_t \leq \epsilon\}$  and  $\tilde{t}_\epsilon \stackrel{\text{def}}{=} \min_t \{t : \tilde{\delta}_t \leq \epsilon\}$ . For any initial function value  $x_0$  s.t.  $\delta_0 > 1, \exists \epsilon_0 \in (0, 1)$  such that  $\forall \epsilon > \epsilon_0, t_\epsilon \geq \tilde{t}_\epsilon$ .

*Proof.* For the gradient flow update on the  $\ell_2$  objective, we have,

$$\frac{d\ell_2(x_t, y)}{dt} = \frac{d\ell_2(x_t, y)}{d\delta_t} \cdot \frac{d\delta_t}{dx_t} \cdot \frac{dx_t}{dt} \quad (5)$$

$$= \delta_t \cdot \text{sgn}(x_t - y) \cdot [-\eta \cdot (x_t - y)] \quad (6)$$

$$= \delta_t \cdot \text{sgn}(x_t - y) \cdot [-\eta \cdot \text{sgn}(x_t - y) \cdot \delta_t] \quad (7)$$

$$= -\eta \cdot \delta_t^2 = -2 \cdot \eta \cdot \ell_2(x_t, y). \quad (8)$$

which implies,

$$\frac{d\{\ln \ell_2(x_t, y)\}}{dt} = \frac{1}{\ell_2(x_t, y)} \cdot \frac{d\ell_2(x_t, y)}{dt} = -2 \cdot \eta. \quad (9)$$

Taking integral, we have,

$$\ln \ell_2(x_t, y) - \ln \ell_2(x_0, y) = -2 \cdot \eta \cdot t, \quad (10)$$

which is equivalent to (letting  $\delta_t = \epsilon$ ),

$$t_\epsilon \stackrel{\text{def}}{=} \frac{1}{2\eta} \cdot \ln \left\{ \frac{\ell_2(x_0, y)}{\ell_2(x_t, y)} \right\} = \frac{1}{\eta} \cdot \ln \left\{ \frac{\delta_0}{\delta_t} \right\} = \frac{1}{\eta} \cdot \ln \left\{ \frac{\delta_0}{\epsilon} \right\}. \quad (11)$$

On the other hand, for the gradient flow update on the  $\ell_3$  objective, we have,

$$\frac{d\ell_3(\tilde{x}_t, y)}{dt} = \frac{d\ell_3(\tilde{x}_t, y)}{d\tilde{\delta}_t} \cdot \frac{d\tilde{\delta}_t}{d\tilde{x}_t} \cdot \frac{d\tilde{x}_t}{dt} \quad (12)$$

$$= \tilde{\delta}_t^2 \cdot \text{sgn}(\tilde{x}_t - y) \cdot [-\eta \cdot \tilde{\delta}_t^2 \cdot \text{sgn}(\tilde{x}_t - y)] \quad (13)$$

$$= -\eta \cdot \tilde{\delta}_t^4 = -3^{\frac{4}{3}} \cdot \eta \cdot (\ell_3(\tilde{x}_t, y))^{\frac{4}{3}}, \quad (14)$$

which implies,

$$\frac{d\{(\ell_3(\tilde{x}_t, y))^{-\frac{1}{3}}\}}{dt} = -\frac{1}{3} \cdot (\ell_3(\tilde{x}_t, y))^{-\frac{4}{3}} \cdot \frac{d\ell_3(\tilde{x}_t, y)}{dt} = 3^{\frac{1}{3}} \cdot \eta. \quad (15)$$

Taking integral, we have,

$$(\ell_3(\tilde{x}_t, y))^{-\frac{1}{3}} - (\ell_3(\tilde{x}_0, y))^{-\frac{1}{3}} = 3^{\frac{1}{3}} \cdot \eta \cdot t, \quad (16)$$

which is equivalent to (letting  $\tilde{\delta}_t = \epsilon$ ),

$$\tilde{t}_\epsilon \stackrel{\text{def}}{=} \frac{1}{3^{\frac{1}{3}} \cdot \eta} \cdot \left[ (\ell_3(\tilde{x}_t, y))^{-\frac{1}{3}} - (\ell_3(\tilde{x}_0, y))^{-\frac{1}{3}} \right] = \frac{1}{\eta} \cdot \left( \frac{1}{\tilde{\delta}_t} - \frac{1}{\delta_0} \right) = \frac{1}{\eta} \cdot \left( \frac{1}{\epsilon} - \frac{1}{\delta_0} \right). \quad (17)$$

Then we have,

$$t_\epsilon - \tilde{t}_\epsilon = \frac{1}{\eta} \cdot \ln \left\{ \frac{\delta_0}{\epsilon} \right\} - \frac{1}{\eta} \cdot \left( \frac{1}{\epsilon} - \frac{1}{\delta_0} \right) \quad (18)$$

$$= \frac{1}{\eta} \cdot \left[ \left( \ln \frac{1}{\epsilon} - \frac{1}{\epsilon} \right) - \left( \ln \frac{1}{\delta_0} - \frac{1}{\delta_0} \right) \right]. \quad (19)$$

Define the function  $f(x) = \ln \frac{1}{x} - \frac{1}{x}$ ,  $x > 0$  is continuous and  $\max_{x>0} f(x) = f(1) = -1$ . We have  $\lim_{x \rightarrow 0} f(x) = \lim_{x \rightarrow \infty} f(x) = -\infty$ , and  $f(\cdot)$  is monotonically increasing for  $x \in (0, 1]$  and monotonically decreasing for  $x \in (1, \infty)$ .

Given  $\delta_0 > 1$ , we have  $f(\delta_0) < f(1) = -1$ . Using the intermediate value theorem for  $f(\cdot)$  on  $(0, 1]$ , we have  $\exists \epsilon_0 < 1$ , such that  $f(\epsilon_0) = f(\delta_0)$ . Since  $f(\cdot)$  is monotonically increasing on  $(0, 1]$  and monotonically decreasing on  $(1, \infty)$ , for any  $\epsilon \in [\epsilon_0, \delta_0]$ , we have  $f(\epsilon) \geq f(\delta_0)$ .<sup>5</sup> Hence we have,

$$t_\epsilon - \tilde{t}_\epsilon = \frac{1}{\eta} \cdot [f(\epsilon) - f(\delta_0)] \geq 0. \quad \square$$

**Remark 1.** Figure 7 shows the function  $f(x) = \ln \frac{1}{x} - \frac{1}{x}$ ,  $x > 0$ . Fix arbitrary  $x' > 1$ , there will be another root  $\epsilon_0 < 1$  s.t.  $f(\epsilon_0) = f(x')$ . However, there is no real-valued solution for  $\epsilon_0$ . The solution in  $\mathbb{C}$  is  $\epsilon_0 = -\frac{1}{W(\log 1/\delta_0 - 1/\delta_0 - \pi i)}$ , where  $W(\cdot)$  is a Wright Omega function. Hence, finding the exact value of  $\epsilon_0$  would require a definition of ordering on complex plane. Our current theorem statement is sufficient for the purpose of characterizing convergence rate. The theorem states that there always exists some desired low error level  $< 1$ , minimizing the square loss converges slower than the cubic loss.

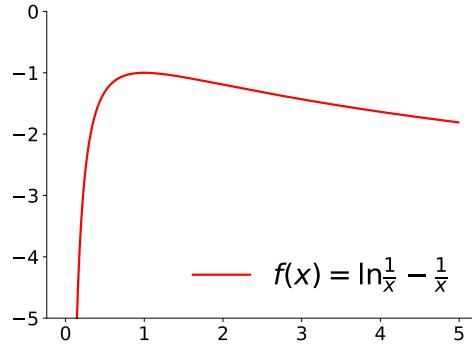


Figure 7: The function  $f(x) = \ln \frac{1}{x} - \frac{1}{x}$ ,  $x > 0$ . The function reaches maximum at  $x = 1$ .

#### A.4 Discussion on the Langevin Dynamics

Define a SDE:  $dW(t) = \nabla U(W_t)dt + \sqrt{2}dB_t$ , where  $B_t \in \mathbb{R}^d$  is a  $d$ -dimensional Brownian motion and  $U$  is a continuous differentiable function. It turns out that the Langevin diffusion  $(W_t)_{t \geq 0}$  converges to a unique invariant distribution  $p(x) \propto \exp(U(x))$  (Chiang et al., 1987). By applying the Euler-Maruyama discretization scheme to the SDE, we acquire the discretized version  $Y_{k+1} = Y_k + \alpha_{k+1} \nabla U(Y_k) + \sqrt{2\alpha_{k+1}} Z_{k+1}$  where  $(Z_k)_{k \geq 1}$  is an i.i.d. sequence of standard  $d$ -dimensional Gaussian random vectors and  $(\alpha_k)_{k \geq 1}$  is a sequence of step sizes. It has been proved that the limiting distribution of the sequence  $(Y_k)_{k \geq 1}$  converges to the invariant distribution of the underlying SDE Roberts (1996); Durmus & Moulines (2017). As a result, considering  $U(\cdot)$  as  $\delta(\cdot)$ ,  $Y$  as  $s$  completes the proof for Theorem 3.

#### A.5 Proof for Theorem 4

We now provide the error bound for Theorem 4. We denote the transition probability distribution under policy  $\pi$  with the true model as  $\mathcal{P}^\pi(r, s' | s)$ ; denote that with the learned model as  $\hat{\mathcal{P}}^\pi(r, s' | s)$ . Let  $p(s)$  and  $\hat{p}(s)$  be the convergent distributions described in Theorem 3 by using true model and learned model respectively. Let  $d_{tv}(\cdot, \cdot)$  be the total variation distance between two probability distributions. Define  $u(s) \stackrel{\text{def}}{=} |\delta(s, y(s))|$ ,  $\hat{u}(s) \stackrel{\text{def}}{=} |\delta(s, \hat{y}(s))|$ ,  $Z \stackrel{\text{def}}{=} \int_{s \in \mathcal{S}} u(s) ds$ ,  $\hat{Z} \stackrel{\text{def}}{=} \int_{s \in \mathcal{S}} \hat{u}(s) ds$ . Then we have the following bound.

<sup>5</sup>Note that  $\epsilon < \delta_0$  by the design of using gradient descent updating rule. If the two are equal,  $t_\epsilon = \tilde{t}_\epsilon = 0$  holds trivially.



**Theorem 4.** Assume: 1) the reward magnitude is bounded  $|r| \leq R_{max}$  and define  $V_{max} \stackrel{\text{def}}{=} \frac{R_{max}}{1-\gamma}$ ; 2) the largest model error for a single state is some small value:  $\epsilon_s \stackrel{\text{def}}{=} \max_s d_{tv}(\mathcal{P}^\pi(\cdot|s), \hat{\mathcal{P}}^\pi(\cdot|s))$ . Then  $\forall s \in \mathcal{S}, |p(s) - \hat{p}(s)| \leq \max(\frac{u(s)+V_{max}\epsilon_s}{Z} - p(s), \frac{\hat{u}(s)+V_{max}\epsilon_s}{Z} - \hat{p}(s))$ .

*Proof.* First, we bound the estimated temporal difference error. Fix an arbitrary state  $s \in \mathcal{S}$ , it is sufficient to consider the case  $u(s) > \hat{u}(s)$ , then

$$\begin{aligned} |u(s) - \hat{u}(s)| &= u(s) - \hat{u}(s) \\ &= \mathbb{E}_{(r,s') \sim \mathcal{P}^\pi} [r + \gamma v^\pi(s')] - \mathbb{E}_{(r,s') \sim \hat{\mathcal{P}}^\pi} [r + \gamma v^\pi(s')] \\ &= \int_{s,r} (r + \gamma v^\pi(s)) (\mathcal{P}^\pi(s', r|s) - \hat{\mathcal{P}}^\pi(s', r|s)) ds' dr \\ &\leq (R_{max} + \gamma \frac{R_{max}}{1-\gamma}) \int_{s,r} (\mathcal{P}^\pi(s', r|s) - \hat{\mathcal{P}}^\pi(s', r|s)) ds' dr \\ &\leq V_{max} d_{tv}(\mathcal{P}^\pi(\cdot|s), \hat{\mathcal{P}}^\pi(\cdot|s)) \leq V_{max} \epsilon_s \end{aligned}$$

Then we take into consideration of the normalizer of the Gibbs distribution. Consider the case  $p(s) > \hat{p}(s)$  first.

$$p(s) - \hat{p}(s) \leq \frac{\hat{u}(s) + V_{max}\epsilon_s}{Z} - \hat{p}(s)$$

This corresponds to the second term in the maximum operation. The first term corresponds to the case  $p(s) < \hat{p}(s)$ . This completes the proof.  $\square$

## A.6 Reproducible Research

Our implementations are based on tensorflow with version 1.13.0 (Abadi et al., 2015). We use Adam optimizer (Kingma & Ba, 2014) for all experiments.

### A.6.1 Reproduce experiments before Section 5

**Supervised learning experiment.** For the supervised learning experiment shown in section 3, we use  $32 \times 32$  tanh units neural network, with learning rate swept from  $\{0.01, 0.001, 0.0001, 0.00001\}$  for all algorithms. We compute the constant  $c$  as specified in the Theorem 1 at each time step for Cubic loss. We compute the testing error every 500 iterations/mini-batch updates and our evaluation learning curves are plotted by averaging 50 random seeds. For each random seed, we randomly split the dataset to testing set and training set and the testing set has 1k data points. Note that the testing set is not noise-contaminated.

**Reinforcement Learning experiments in Section 3.** We use a particularly small neural network  $16 \times 16$  to highlight the issue of incomplete priority updating. Intuitively, a large neural network may be able to memorize each state’s value and thus updating one state’s value is less likely to affect others. We choose a small neural network, in which case a complete priority updating for all states should be very important. We set the maximum ER buffer size as 10k and mini-batch size as 32. The learning rate is 0.001 and the target network is updated every 1k steps.

**Distribution distance computation in Section 4.** We now introduce the implementation details for Figure 3. The distance is estimated by the following steps. First, in order to compute the desired sampling distribution, we discretize the domain into  $50 \times 50$  grids and calculate the absolute TD error of each grid (represented by the left bottom vertex coordinates) by using the true environment model and the current learned  $Q$  function. We then normalize these priorities to get probability distribution  $p^*$ . Note that this distribution is considered as the desired one since we have access to all states across the state space with priorities computed by current Q-function at each time step. Second, we estimate our sampling distribution by randomly sampling 3k states from search-control queue and count the number of states falling into each discretized grid and normalize these counts to get  $p_1$ . Third, for comparison, we estimate the sampling distribution of the conventional prioritized ER (Schaul et al., 2016) by sampling 3k states from the prioritized ER buffer and count the states falling into each grid and compute its corresponding distribution  $p_2$  by normalizing the counts.

Then we compute the distances of  $p_1, p_2$  to  $p^*$  by two weighting schemes: 1) on-policy weighting:  $\sum_{j=1}^{2500} d^\pi(s_j) |p_i(s_j) - p^*(s_j)|, i \in \{1, 2\}$ , where  $d^\pi$  is approximated by uniformly sample 3k states from a recency buffer and normalizing their visitation counts on the discretized GridWorld; 2) uniform weighting:  $\frac{1}{2500} \sum_{j=1}^{2500} |p_i(s_j) - p^*(s_j)|, i \in \{1, 2\}$ . We examine the two weighting schemes because of two considerations: for the on-policy weighting, we concern about the asymptotic convergent behavior and want to down-weight those states with relatively high TD error but get rarely visited as the policy gets close to optimal; uniform weighting makes more sense during early learning stage, where we consider all states are equally important and want the agents to sufficiently explore the whole state space.

## A.6.2 Reproduce experiments in Section 5

For our algorithm, the pseudo-code with concrete parameter settings is presented in Algorithm 4.

**Common settings.** For all domains other than roundabout-v0, we use  $32 \times 32$  neural network with ReLu hidden units except the Dyna-Frequency which uses tanh units as suggested by the author (Pan et al., 2020).<sup>6</sup> Except the output layer parameters which were initialized from a uniform distribution  $[-0.003, 0.003]$ , all other parameters are initialized using Xavier initialization (Glorot & Bengio, 2010). We use mini-batch size  $b = 32$  and maximum ER buffer size 50k. All algorithms use target network moving frequency 1000 and we sweep learning rate from  $\{0.001, 0.0001\}$ . We use warm up steps = 5000 (i.e. random action is taken in the first 5k time steps) to populate the ER buffer before learning starts. We keep exploration noise as 0.1 without decaying.

**Meta-parameter settings.** For our algorithm Dyna-TD, we are able to keep the same parameter setting across all benchmark domains:  $\alpha_a = 0.1, c = 20$  and learning rate 0.001. For all Dyna variants, we fetch the same number of states ( $m = 20$ ) from hill climbing (i.e. search-control process) as Dyna-TD does, and use  $\epsilon_a = 0.1$  and set the maximum number of gradient step as  $k = 100$  unless otherwise specified.

Our Prioritized ER is implemented as the proportional version with sum tree data structure. To ensure fair comparison, since all model-based methods are using mixed mini-batch of samples, we use prioritized ER without importance ratio but half of mini-batch samples are uniformly sampled from the ER buffer as a strategy for bias correction. For Dyna-Value and Dyna-Frequency, we use the setting as described by the original papers.

For the purpose of learning an environment model, we use a  $64 \times 64$  ReLu units neural network to predict  $s' - s$  and reward given a state-action pair  $s, a$ ; and we use mini-batch size 128 and learning rate 0.0001 to minimize the mean squared error objective for training the environment model.

**Environment-specific settings.** All of the environments are from OpenAI (Brockman et al., 2016) except that: 1) the GridWorld environment is taken from Pan et al. (2019) and the MazeGridWorld is from Pan et al. (2020); 2) Roundabout-v0 is from Laurent et al. (2019). For all OpenAI environments, we use the default setting except on Mountain Car where we set the episodic length limit to 2k. The GridWorld has state space  $\mathcal{S} = [0, 1]^2$  and each episode starts from the left bottom and the goal area is at the top right  $[0.95, 1.0]^2$ . There is a wall in the middle with a hole to allow the agent to pass. MazeGridWorld is a more complicated version where the state and action spaces are the same as GridWorld, but there are two walls in the middle and it takes a long time for model-free methods to be successful. On the this domain, we use the same setting as the original paper for all Dyna variants. We use exactly the same setting as described above except that we change the  $Q$ -network size to  $64 \times 64$  ReLu units, and number of search-control samples is  $m = 50$  as used by the original paper. We refer readers to the original paper (Pan et al., 2020) for more details.

On roundabout-v0 domain, we use  $64 \times 64$  ReLu units for all algorithms and set mini-batch size as 64. For Dyna-TD, we start using the model after 5k steps and set  $m = 100, \alpha_a = 1.0, k = 500$  and we do search-control every 10 environment time steps to reduce computational cost. To alleviate the effect of model error, we use only 16 out of 64 samples from the search-control queue in a mini-batch.

<sup>6</sup>Note that this is one of its disadvantages: the search-control of Dyna-Frequency requires the computation of Hessian-gradient product and it is empirically observed that the Hessian is frequently zero when using ReLu as hidden units (Pan et al., 2020).

---

**Algorithm 3** Dyna-TD

---

**Input:**  $m$ : number of states to fetch through search-control;  $B_{sc}$ : empty search-control queue;  $B_{er}$ : ER buffer;  $\epsilon_a$ : threshold for accepting a state; initialize  $Q$ -network  $Q_\theta$

**for**  $t = 1, 2, \dots$  **do**

  Observe  $(s_t, a_t, s_{t+1}, r_{t+1})$  and add it to  $B_{er}$

  // Hill climbing on absolute TD error

  Sample  $s$  from  $B_{er}$ ,  $c \leftarrow 0$ ,  $\tilde{s} \leftarrow s$

**while**  $c < m$  **do**

$\hat{y} \leftarrow \mathbb{E}_{s', r \sim \hat{P}(\cdot|s, a)}[r + \gamma \max_a Q_\theta(s', a)]$

    Update  $s$  by rule (3)

**if**  $s$  is out of the state space **then**

      Sample  $s$  from  $B_{er}$ ,  $\tilde{s} \leftarrow s$  // restart

**continue**

**if**  $\|\tilde{s} - s\|_2 / \sqrt{d} \geq \epsilon_a$  **then**

      //  $d$  is the number of state variables, i.e.  $\mathcal{S} \subset \mathbb{R}^d$

      Add  $s$  into  $B_{sc}$ ,  $\tilde{s} \leftarrow s$ ,  $c \leftarrow c + 1$

  //  $n$  planning updates

**for**  $n$  times **do**

    Sample a mixed mini-batch with half samples from  $B_{sc}$  and half from  $B_{er}$

    Update  $Q$ -network parameters by using the mixed mini-batch

---

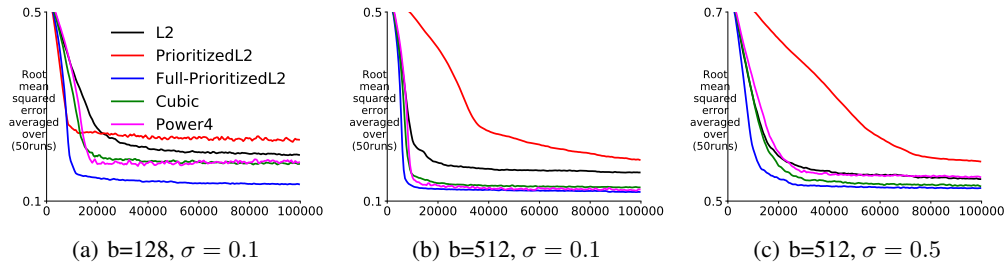


Figure 8: Figure(a)(b)(c) show the training RMSE as a function of number of mini-batch updates with different mini-batch sizes or Gaussian noises with different  $\sigma$  added to the training targets. The results are averaged over 50 random seeds. The standard error is small enough to get ignored.

## A.7 Additional Experiments

The main purpose of the additional experiments here is to strengthen our claims from Section 3.

**Learning curve in terms of training error corresponding to Figure 2.** In Section 3.1, we show the learning curve in terms of testing error. We now show training error to closely match our theoretical result 1. As a supplement, we include the learning curve in terms of testing error in Figure 8.

**Learning curve with a larger neural network on the sin dataset.** We try to eliminate the effect of neural network size. Hence we use a larger neural network size ( $128 \times 128$  tanh units) on the same sin dataset. As one can see from Figure 9, FullPrioritizedL2 still performs the best and when we increase the mini-batch size from 128 to 512, the high power objective versions still moves closer to FullPrioritizedL2, as we saw in Figure 2.

**Learning curve with on a real-world dataset.** To illustrate the generality of our Theorem 1, we also conduct tests on a frequently cited regression *Bike sharing dataset* Fanaee-T & Gama (2013). The data preprocessing is as follows. We remove attributes: date, index, year, weather situation 4, weekday 7, registered, casual. We use one-hot encoding for all categorical variables. We scale the target to  $[0, 1]$  and scale it back when computing training errors. We use a  $64 \times 64$  ReLU units neural network with mini-batch size 128 and learning rate 0.0001 for training.

It should be noted that the behavior of Cubic is consistent on the previous sin example and on this real world dataset: it gets closer to FullPrioritizedL2 as we increase the mini-batch size. Another

---

**Algorithm 4** Dyna-TD with implementation details

---

**Input or notations:**  $k = 20$ : number search-control states to acquire by hill climbing,  $k_b = 100$ : the budget of maximum number of hill climbing steps;  $\rho = 0.5$ : percentage of samples from search-control queue,  $d : \mathcal{S} \subset \mathbb{R}^d$ ; empty search-control queue  $B_{sc}$  and ER buffer  $B_{er}$   
empirical covariance matrix:  $\hat{\Sigma}_s \leftarrow \mathbf{I}$   
 $\mu_{ss} \leftarrow \mathbf{0} \in \mathbb{R}^{d \times d}, \mu_s \leftarrow \mathbf{0} \in \mathbb{R}^d$  (auxiliary variables for computing empirical covariance matrix, sample average will be maintained for  $\mu_{ss}, \mu_s$ )  
 $n_\tau \leftarrow 0$ : count for parameter updating times,  $\tau \leftarrow 1000$  target network updating frequency  
 $\epsilon_a \leftarrow 0$ : threshold for accepting a state  
Initialize  $Q$  network  $Q_\theta$  and target  $Q$  network  $Q_{\theta'}$   
**for**  $t = 1, 2, \dots$  **do**  
  Observe  $(s, a, s', r)$  and add it to  $B_{er}$   
   $\mu_{ss} \leftarrow \frac{\mu_{ss}(t-1) + ss^\top}{t}, \mu_s \leftarrow \frac{\mu_s(t-1) + s}{t}$   
   $\hat{\Sigma}_s \leftarrow \mu_{ss} - \mu_s \mu_s^\top$   
   $\epsilon_a \leftarrow (1 - \beta)\epsilon_a + \beta \|s' - s\|_2$  for  $\beta = 0.001$   
  // Hill climbing on absolute TD error  
  Sample  $s$  from  $B_{er}, c \leftarrow 0, \tilde{s} \leftarrow s, i \leftarrow 0$   
  **while**  $c < k$  and  $i < k_b$  **do**  
    // since environment is deterministic, the environment model becomes a Dirac-delta distribution and we denote it as a deterministic function  $\mathcal{M} : \mathcal{S} \times \mathcal{A} \mapsto \mathcal{S} \times \mathbb{R}$   
     $s', r \leftarrow \mathcal{M}(s, a)$   
     $\hat{y} \leftarrow r + \gamma \max_a Q_\theta(s', a)$   
    // add a smooth constant  $10^{-5}$  inside the logarithm  
     $s \leftarrow s + \alpha_a \nabla_s \log(|\hat{y} - \max_a Q(s, a; \theta_t)| + 10^{-5}) + X, X \sim N(0, 0.01 \hat{\Sigma}_s)$   
    **if**  $s$  is out of the state space **then**  
      // restart hill climbing  
      Sample  $s$  from  $B_{er}, \tilde{s} \leftarrow s$   
    **continue**  
    **if**  $\|\tilde{s} - s\|_2 / \sqrt{d} \geq \epsilon_a$  **then**  
      Add  $s$  into  $B_{sc}, \tilde{s} \leftarrow s, c \leftarrow c + 1$   
     $i \leftarrow i + 1$   
  **for**  $n$  times **do**  
    Sample a mixed mini-batch  $b$ , with proportion  $\rho$  from  $B_{sc}$  and  $1 - \rho$  from  $B_{er}$   
    Update parameters  $\theta$  (i.e. DQN update) with  $b$   
     $n_\tau \leftarrow n_\tau + 1$   
    **if**  $\text{mod}(n_\tau, \tau) == 0$  **then**  
       $Q_{\theta'} \leftarrow Q_\theta$

---

observation is that the Power4 objective is highly variant on this domain, because the real world data should be noisy and the high order objective suffers. This observation corresponds to what we observed in Section 3.1, where we show that high power objective is sensitive to the noise.

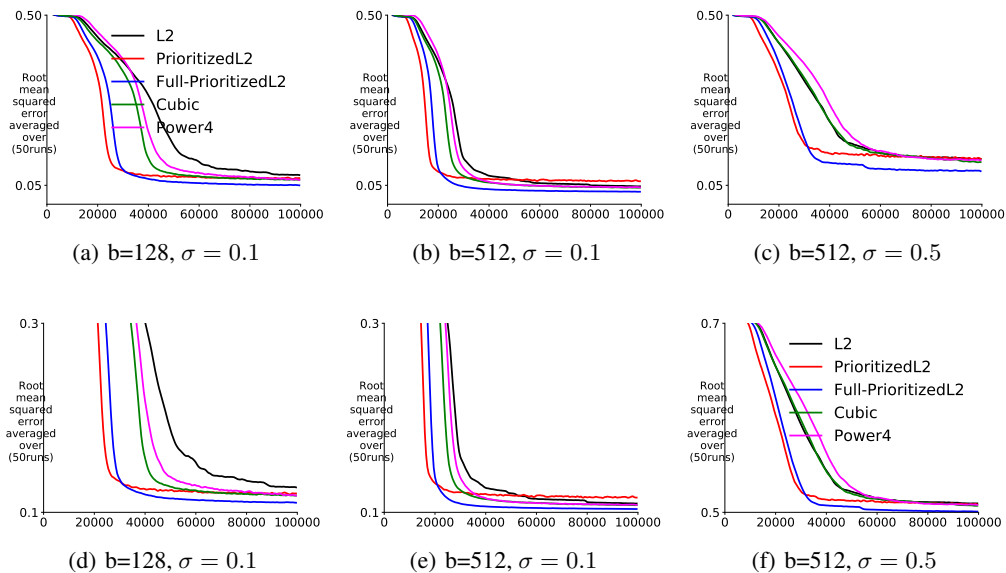


Figure 9: Figure(a)(b)(c) show the testing RMSE as a function of number of mini-batch updates with different mini-batch sizes or Gaussian noises with different  $\sigma$  added to the training targets. (d)(e)(f) show the training RMSE. The results are averaged over 50 random seeds. The standard error is small enough to get ignored. Note that the target variable in the testing set is not noise-contaminated.

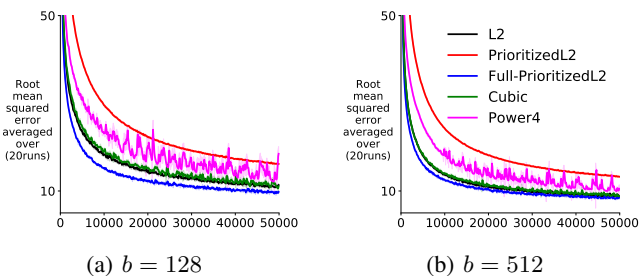


Figure 10: Figure(a)(b)(c) show the training RMSE as a function of number of mini-batch updates on the Bike sharing dataset. The results are averaged over 20 random seeds. The shade indicates standard error.